

Response to Reviewer 1

We thank the reviewer for the insightful comments and for noting some important corrections. As detailed in the following, we have revised the paper in accordance with each point. Detailed changes are indicated in the highlighted manuscript uploaded with this response. Here, reviewer comments are in blue text and our responses are in black text.

This paper investigates if cloud parcels that go through a mixing event can produce larger droplets than undisturbed parcels (this is called super-adiabatic growth by the authors). Mixed parcels contain less water and fewer droplets than undisturbed parcels, and therefore droplets there grow faster after a mixing event, although starting from a smaller radius. From thermodynamical considerations, the authors show that super-adiabatic growth is expected for a pristine environment when mixed parcels rise to a given height. This height mostly depends on the thermodynamical properties of the cloud and of the environment, and it is independent of the updraft velocity and of the mixing fraction. This result is tested with a parcel model for different updrafts velocities, different polluted environments and for a polydisperse droplet population.

It has been argued in the past that super-adiabatic droplet growth can help to explain rain formation in warm clouds. The authors are able to quantify this effect in idealized conditions, and I think that their results can be used to estimate the relevance of the mechanism in future studies. For these reasons, I think that the work can be a worthy publication for ACP if the authors answer the next questions.

1) One of the inherent assumptions for the parcel model and for the thermodynamical calculations is that the parcel only mixes once with the cloud-free environment, which means that it never mixes with cloudy air. I would like that the authors discuss this assumption more in detail. Clouds are turbulent and continuously mix (see for example Margaritz et al. 2014), which homogenizes the droplet number concentration. In the example from Figure 1, the parcel has to rise for ~3000 seconds without mixing with other cloud parcels in order to become super adiabatic. It seems unlikely for me to find such a parcel in a real cloud.

This comment is of course correct, and the reviewer is right to request further justification of our idealized approach. As stated in the reviewer comment, a cloud parcel continuously mixes with both cloudy air and the environment air throughout its trajectory. Lagrangian results such as those of Margaritz et al. 2014 and others (e.g., several already cited in the paper, including Cooper et al. 2013, de Lozar and Muessle 2016, Lasher-Trapp et al. 2005, Margaritz et al. 2015, and Naumann and Seifert 2015) have demonstrated some effects of internal mixing, especially due to sedimentation when drizzle is present, and that dilution events often take place repeatedly during parcel ascent. The results presented here do not consider those more realistic conditions, but instead are purposefully designed so as to avoid the complexity of a real cloud and look at the idealized response to a single dilution event. Our motivating philosophy is that if we can understand the ‘impulse response’ from one mixing event with analytical results, then that understanding can be extended to more complex scenarios. The main purpose of this paper is therefore to study how the cloud microphysical properties in a diluted parcel change when it rises adiabatically after the mixing event, and indeed the derived results are shown to be consistent

with a more detailed (yet still idealized) parcel model. The analytical results might be useful to calculate the entrainment rate profile for the real cloud, similar to Lu et al. (2012), for example. We have added more discussion in the introduction to motivate our idealized approach and how it can be placed in context with more complex, real cloud turbulence. As part of that discussion we include a citation to Magaritz et al. (2014), as well as to several other papers that draw attention to the microphysical effects of internal and external mixing (Korolev et al. 2013, Wang et al. 2009).

2) It would be interesting to know the authors conclusions about the role of super adiabatic droplets for large droplets production and rain formation, from the results presented in the paper. Do they think that the mechanism is relevant for all warm clouds or only in a few particular cases (very wet and very clean environment)? Do they think that the mechanism is relevant for stratocumulus (which are usually thin (~300 m), with a dry capping free atmosphere and with mixing only on the top)? Can they estimate how does the droplet size distribution broaden due to this mechanism (is it sufficient for rain formation)?

Our results show that a mixed/diluted parcel is more likely to reach the superadiabatic growth region if the environmental air is wet and clean. This mechanism might be relevant not only for cumulus, but also for stratocumulus cloud. For example, as mentioned by reviewer 2, Wang et al. (2009) describe a circulation mixing hypothesis to explain microphysical properties in stratocumulus clouds. The circulation mixing hypothesis is similar in spirit to the assumption in our study, except it is conceptually dependent on multiple dilution events and therefore somewhat more qualitative. The circulation hypothesis of Korolev et al. (2013) also has some similarities and is able to produce large droplets that, by our definition would be considered superadiabatic. Our results focus on the possibility of enhanced growth of cloud droplets when they enter the superadiabatic growth region. When those enhanced-growth cloud droplets are mixed with other cloud parcels, the size distribution will be broadened, and while we mentioned this possibility, we have not quantified the broadening effect. This is definitely a key topic that needs to be the focus of future research. We have added some discussion of these points in the introduction and discussion sections.

Technical corrections:

1) Line 120. Equation (4) can be directly obtained from Eq. (1) in the quasi-stationary limit. No need to refer to Eqs. (2) and (3).

Thanks for the reviewer's comment. Yes Equation 4 can be obtained from Equation 1 and we have reordered the equations to make this clear. Because quasi-stationary supersaturation (former Equation 2) is used to explain the enhanced growth of cloud droplet in the mixing parcel, we still keep it.

2) Line 135. There is a prefactor missing in the definition of the liquid potential temperature, which accounts for the pressure dependence. With the current definition, liquid potential temperature is only conserved for adiabatic and isobaric processes. Also, I do not see why ϵ appears in the definition (it does not appear in Gerber et al. 2008).

Thanks for the reviewer's comment. Yes, we didn't consider the pressure effect on liquid potential temperature. This assumption works if the cloud is not thick. We add more discussion in the text. Because the unit of lw is J/mol (not J/kg) and the unit of cp is J/mol/K (not J/kg/K) (see Appendix), ϵ is a constant to change the unit of lw to J/kg, and change the unit of cp to J/kg/K. Our unit is not as usual as previous paper, but it's consistent in our paper and consistent with that in Lamb and Verlinde's textbook. There were no errors and our results were correct. Since both reviewers were confused by the notation, however, we have changed to the mass-based units in the text since this is the most common terminology.

3) Line 141. Equation number missing.

We've added the equation number in Line 141.

4) Line 151. I would not discuss the state im (after mixing but before phase changes). It is not very useful for the discussion, and it adds more symbols.

We've removed $q_{v,im}$ and T_{im} in the text.

5) Line 156 and 192. Equation 2.1 does not exist.

Equation 2.1 should be Equation 6 (former Equation 7). We've changed it in the text.

6) Line 246. Explain better why $q_{l,fm}/q_{l,f} = \chi$ is the condition for the critical height. Remind the condition of completely clean environment.

This condition only works for the cloud parcel with monodisperse cloud droplet when mixing with clean environment. For a clean environment and homogeneous mixing, it's true that $n_{d,fm}/n_{d,f} = \chi$ as long as droplets in the mixing parcel don't totally evaporate. Here n_d means the cloud droplet number concentration. For monodisperse cloud droplet, if $q_{l,fm}/q_{l,f}$ also equals to χ , it means that the droplet sizes in both mixing and original parcels are the same. Because $q_l = \frac{4}{3}\pi \rho_l r^3 N_d$. More explanation is added to explain the condition for the critical height.

7) Line 316. Provide the number of CCN in the polluted environment.

For the polluted case, the dry aerosol distribution in the environment is the same as that below the cloud. The total number concentration of aerosol is 50 #/g. The number of cloud droplet can be seen in the new Figures in the supplementary material.

Finally, we have slightly edited the abstract for concision and clarity in accordance with the implemented changes.

Response to Reviewer 2

We thank the reviewer for the insightful comments and for noting some important corrections. As detailed in the following, we have revised the paper in accordance with each point. Detailed changes are indicated in the highlighted manuscript uploaded with this response. Here, reviewer comments are in blue text and our responses are in black text.

In this manuscript the authors tried to tackle the problem of super-adiabatic droplet growth, which has been a subject of great interest in cloud physics community for the last several decades. For without such growth, warm rain initiation within a realistic time scale seems very difficult, if not impossible. The authors considered entrainment and mixing processes as a key to the super-adiabatic droplet growth and derived equations that could calculate analytically the variation of temperature and liquid water mixing ratio and thus droplet radius after entrainment and mixing and during the further ascent of the mixed cloud parcel. Then the authors demonstrated that this theoretical formulation was consistent with the results of cloud parcel model simulations of such processes. Moreover, the authors suggested some proper environmental conditions for super-adiabatic droplet growth. This manuscript does add some new insights on super-adiabatic droplet growth and could be worth publication in ACP if the following issues are handled properly.

In Eq. (7), epsilon appears in the denominator of the second term in each side, which is not right. Likewise, epsilon in Eq. (15) should be removed. A critical mistake is made in Eq. (12): pf in the denominator of the right hand side should be removed. Meanwhile, in Eq. (14), pf should appear in the denominator of the second term on the right hand side. I doubt that these wrong formulations were actually used in theoretical calculations. If that was the case, the results might have been very different from those shown in the manuscript. The authors should clear this problem.

We appreciate that the reviewer has checked our equations carefully. For Eq. (7) (now it's Eq. 6), epsilon in fact should be there because we were using molar rather than mass units: the units of lw are J/mol (not J/kg) and the units of c_p are J/mol/K (not J/kg/K). Epsilon is a constant to change the units of lw to J/kg, and to change the units of c_p to J/kg/K. Our units are not as typical as in some previous papers, but are consistent within our paper and are consistent with those in Lamb and Verlinde's widely used textbook. There were no errors and our results were correct, but since both reviewers were confused by it, we have changed to the mass-based units in the text since this is the most common terminology.

In Eq. (12) and (14) (now they are Eq. 11 and 13), there are indeed some typos. As the reviewer stated, pf should not be in Eq. (12) but should appear in the denominator of the second term on the right hand side. Our final results (Eq.15-18) are correct, however. The constant C_2 is actually from the last term of Eq. (14), and pf exists in C_2 (see Appendix).

The authors used a cloud parcel model to calculate the evolution of cloud droplet size distribution during the ascent of a cloud parcel after entrainment and mixing. Very similar but much more sophisticated calculations were already made by Wang et al. (2009). Using a cloud parcel model that incorporates a full CCN spectrum, they calculated the evolution of cloud

droplet distribution in an ascending cloud parcel that was mixed with just saturated air in several different proportions. Because the mixed air was just saturated, classification of homogeneous or inhomogeneous mixing was irrelevant. However, during the ascent after mixing, supersaturation of the mixed cloud parcel was readjusted and droplet number concentration and size distribution responded accordingly. Right after mixing, mean droplet diameter was reduced due to the newly activated small droplets from the portion of the just saturated air, but because of reduced droplet number concentration, droplet growth was faster and eventually at some altitude above the mean diameter of the mixed cloud parcel became larger than that of the unmixed cloud parcel. Here the key to the faster droplet growth was due to reduced droplet number concentration and increased supersaturation in the mixed cloud parcel after just saturated air was mixed. Such behavior cannot be resolved when a monodisperse CCN distribution is used as was done in Figs. 1 and 2. But for Fig. 3, a polydisperse CCN distribution was used and the evolution of individual size classes was calculated. Similarly to Wang et al. (2009), I urge the authors to show the variation of supersaturation and activated droplet number concentration and to include them in the discussion of faster growth in the mixed cloud parcel.

We thank the reviewer for bringing our attention to the very interesting work of Wang et al. (2009). It does have some common aspects and we have added discussion of those aspects to our paper. As requested, we have generated figures that show the variation of supersaturation and the activated droplet number concentration for all cases in our paper. We agree that they are useful to include for those readers who are interested in the details. Because this would nearly double the number of figures in this short paper and because they are not completely focused on the central message of super-adiabatic droplet growth, we propose that they be included in an online supplement where readers interested in these quantities can easily access them. The variation of supersaturation and activated droplet number concentration profiles are mentioned in the text with a reference to the supplemental figures.

Obviously the mixing scenario presented in this manuscript is not likely to occur in exactly the same manner in real clouds. As pointed out by the authors, inhomogeneous mixing may occur instead of homogeneous mixing. Cloud parcels may undergo multiple mixing events not only with entrained environmental air but also with neighboring in-cloud parcels as exemplified in Wang et al. (2009). Some discussion should be made in this perspective.

Thanks for the reviewer's comment. Reviewer 1 also raised a similar point and we have added a more thorough discussion of mixing with neighboring in-cloud parcels in the discussion section.

Line 47: one of 'that' should be removed.

We've removed one 'that'.

Line 192: Equation 2.1 does not exist. Apparently it is meant to be Equation 7.

We've changed it to Eq. 6 (former Eq. 7).

Line 320: The fact that more aerosols lead to smaller cloud droplets is simply a fundamental aspect of cloud physics. This does not indicate aerosol indirect effect. The key factor of aerosol indirect effect is the anthropogenic increase of aerosol concentration that leads to increased

concentration of smaller cloud droplets. So linking the fact that more aerosols lead to smaller cloud droplets to aerosol indirect effect is not appropriate.

Yes, we agree with the reviewer's point and have removed that sentence.

Where is Table 1? I only see Table 2.

Table 1 was in the Appendix. To avoid any confusion, and because those results are not critical for the main flow of the paper, we now have moved Table 2 to the online supplementary material.

Finally, we have slightly edited the abstract for concision and clarity in accordance with the implemented changes.

Conditions for super-adiabatic droplet growth after entrainment mixing

Fan Yang¹, Raymond Shaw¹, and Huiwen Xue²

¹Atmospheric Sciences Program and Department of Physics, Michigan Technological University, Houghton, Michigan

²Department of Atmospheric and Oceanic Sciences, School of Physics, Peking University, Beijing, China

Correspondence to: Raymond Shaw (rashaw@mtu.edu)

Abstract. Cloud droplet response to entrainment and mixing between a cloud and its environment is considered, accounting for subsequent droplet growth during adiabatic ascent following a mixing event. The vertical profile for liquid water mixing ratio after a mixing event is derived analytically, allowing the reduction to be predicted from the mixing fraction and from the temperature and humidity for both the cloud and environment. It is derived for the limit of homogeneous mixing. The expression leads to a critical height above the mixing level: At the critical height the cloud droplet radius is the same for both mixed and unmixed parcels, and the critical height is independent of the updraft velocity and mixing fraction. Cloud droplets in a mixed parcel are larger than in an unmixed parcel above the critical height, which we refer to as the “super-adiabatic” growth region. Analytical results are confirmed with a bin microphysics cloud model. Using the model, we explore the effects of updraft velocity, aerosol source in the environmental air, and polydisperse cloud droplets. Results show that the mixed parcel is more likely to reach the super-adiabatic growth region when the environmental air is humid and clean. It is also confirmed that the analytical predictions are matched by the volume-mean cloud droplet radius for polydisperse size distributions. The findings have implications for the origin of large cloud droplets that may contribute to onset of collision-coalescence in warm clouds.

1 Introduction

Warm clouds play an important role for the water cycle and energy balance in the atmosphere. However their formation, development and precipitation processes, are still not fully understood (e.g., Beard and Ochs III, 1993). Observations show that warm clouds can precipitate within 20 minutes (e.g., Laird et al., 2000; Göke et al., 2007). One open question is how small cloud droplets, which are on the order of 10 μm , change to rain drops, usually of order 1 mm, within such a short time. Because condensation growth is slow for droplet size larger than approximately 20 μm , collision growth is

believed to be the most important mechanism for warm cloud precipitation (Pruppacher et al., 1998).

25

However, collision efficiency is very low for droplets smaller than $r \approx 30 \mu\text{m}$ due to hydrodynamic interaction. For example, Hocking (1959) considered two moving droplets in the Stokes flow approximation, and found that the collision efficiency for a $r = 19 \mu\text{m}$ droplet with smaller droplets is mostly less than 0.1, and even for a $r = 30 \mu\text{m}$ droplet it is mostly less than 0.5. Such low collision efficiency suppresses the time required for drizzle and precipitation formation. Therefore, large cloud droplets are needed to efficiently initiate precipitation. There are several hypotheses to explain the formation of large cloud droplets: For example, the stochastic collision process itself may produce a small number of “lucky” droplets with larger growth rates (Kostinski and Shaw, 2005). Another possible mechanism is due to the giant cloud condensation nuclei. Observational results show that giant and ultragiant CCNs often exist in the atmosphere, and simulation results indicate that they can be sufficient to start the rain precipitation (e.g., Johnson, 1982; Feingold et al., 1999; Yin et al., 2000; Blyth et al., 2003; Jensen and Lee, 2008; Cheng et al., 2009). But in this paper we focus on mechanisms involving the condensation process. For example, results from Lagrangian tracking studies suggest that large droplets from condensation growth within parcels having favored trajectories can trigger collisions and drizzle formation in warm clouds (Lasher-Trapp et al., 2005; Cooper et al., 2013; Magaritz-Ronen et al., 2014, 2015; Naumann and Seifert, 2015; Lozar and Muessle, 2016). Korolev et al. (2013) proposed that droplet size distribution can be broadened through diffusion growth due to cloud base mixing and vertical fluctuation. Perhaps counter-intuitively, the mixing and entrainment that occurs during cloud evolution itself may be responsible for generating large cloud droplets (Baker et al., 1980). The possibility that that entrainment and subsequent growth can lead to droplets larger than would occur in an unmixed parcel has occupied the attention of the cloud physics community for several decades (e.g., Baker et al., 1980; Jensen et al., 1985; Paluch and Knight, 1986; Su et al., 1998; Cooper et al., 2013; Schmeissner et al., 2015).

Observational results show that the number concentration of cloud droplets at the cloud edge/top is usually smaller than that in the cloud due to entrainment and mixing with environmental air. However, the mean size of cloud droplet at the edge/top might be smaller, equal to, or even larger than that in the cloud (e.g., Burnet and Brenguier, 2007; Lehmann et al., 2009; Lu et al., 2013; Beals et al., 2015), which is thought to be the result of different mixing processes. Baker et al. (1980) proposed two limiting mixing processes: homogeneous and extreme inhomogeneous mixing. Theoretically, mean cloud droplet size will decrease for homogeneous mixing, but remains the same for extreme inhomogeneous mixing. However the actual mixing process near the cloud edge/top and the response of cloud droplets to the mixing process are still unclear. Recently, considerable theoretical and computational work has been directed toward understanding the evolution of the droplet size distribution during both homogeneous and inhomogeneous mixing processes (Andrejczuk et al., 2009;

60

Kumar et al., 2014; Tölle and Krueger, 2014; Korolev et al., 2015; Pinsky et al., 2015b, a). Most of these analyses, however, did not consider the subsequent vertical movement of the mixed parcel, which is also relevant to the evolution of cloud droplets (Wang et al., 2009; Yum et al., 2015; Chen et al., 2015). Finally, most theoretical work thus far does not account for the possibility of secondary
65 activation of aerosols after dilution and mixing, although there is compelling experimental evidence that this occurs (Burnet and Brenguier, 2007; Schmeissner et al., 2015).

In this study, we are interested in the change of cloud microphysical properties after isobaric mixing of cloudy and clear-air volumes, assuming the mixing parcel rises adiabatically afterwards.
70 **In reality, a cloud parcel can continuously mix with both cloudy air and the environment air throughout its trajectory. Previous studies (e.g., (Cooper et al., 2013; Magaritz-Ronen et al., 2014)) have demonstrated some effects of internal mixing, especially due to sedimentation when drizzle is present, and that dilution events often take place repeatedly during parcel ascent. The results presented here do not consider the fully realistic conditions, but instead are**
75 **purposefully designed so as to avoid the complexity of a real cloud and look at the idealized response to a single dilution event. Our motivating philosophy is that if we can understand the ‘impulse response’ from one mixing event with analytical results, then that understanding can be extended to multiple dilution events.** This view of a single mixing event followed by isolated growth is therefore an idealization that allows us to understand the microphysical response in the
80 simplest of conditions. We pose the question, is it possible to achieve “super-adiabatic” droplet diameters as a result of mixing? By super-adiabatic, we mean that the droplet diameter is larger than that observed for an unmixed, closed parcel that grows according to moist-adiabatic conditions (as defined, for example, by Cotton et al. (2011, , Chap. 4)). Specifically, we look for the conditions, such as mixing fraction, ambient humidity, aerosol entrainment, secondary activation, and vertical
85 displacement above the mixing level, that influence the ability to produce larger droplets than exist in an unmixed parcel. We first address the problem by deriving analytical results in Section 2, and then evaluate the theory and explore conditions for super-adiabatic droplet growth using a microphysical cloud parcel model in Section 3. Implications are discussed and results are summarized in Section 4.

90 **2 Analytical results**

As in previous studies, we consider the final state of the microphysical variables (e.g., liquid water mixing ratio, droplet sizes) after homogeneous mixing (e.g., Korolev et al., 2015). This corresponds to the limit of instantaneous mixing, under which conservation of energy and mass result in a unique dependence of droplet size on the mixing fraction (e.g., Andrejczuk et al., 2006; Burnet and Brenguier, 2007; Gerber et al., 2008; Kumar et al., 2014). Here, we consider the similar two stages of
95

homogeneous mixing process as discussed in (Pinsky et al., 2015b), except that the cloud parcel has continuous vertical movement after the mixing event. The first stage is (instantaneous) isobaric mixing in the absence of phase transitions, and the second stage is the response of the droplets in a vertically moving adiabatic (i.e., closed) parcel. Analytical results in this section are derived under the following assumptions: 1) only liquid exists in the condensed form (no ice); 2) the cloud parcel rises adiabatically; 3) the droplet size distribution is monodisperse; 4) the growth of droplets is due to water vapor condensation; 5) sedimentation and collision–coalescence of droplets are ignored.

2.1 Liquid water mixing ratio in an adiabatic cloud without mixing

For reference, we begin by deriving the change of liquid water mixing ratio in a rising adiabatic cloud parcel without mixing. Considering a warm cloud parcel with monodisperse cloud droplets rising adiabatically with a constant updraft velocity, the supersaturation development equation is (Lamb and Verlinde, 2011, p. 417)

$$\frac{ds}{dt} = Q_1 w - Q_2 \frac{dq_l}{dt}, \quad (1)$$

where s is supersaturation, w is updraft velocity, and q_l is the liquid water mixing ratio (g kg^{-1}). Q_1 and Q_2 depend on temperature, pressure and other constants (all symbols and expressions are given in the Appendix). The first term on the right side represents the production of supersaturation due to adiabatic cooling due to vertical displacement, while the second term accounts for the supersaturation depletion due to vapor condensation. For monodisperse cloud droplets $q_l = (4/3)\pi\rho_w r_d^3 n_d$ where r_d is the radius of cloud droplet and n_d is number concentration in units of kg^{-1} . Thus, $dq_l/dt = 4\pi\rho_w n_d r_d^2 dr_d/dt = 4\pi\rho_w n_d r_d G s$. Here we use the linear growth for an individual droplet: $r_d dr_d/dt = G s$, where G is the condensation growth parameter (see Appendix).

By setting the production and depletion terms on the right side of Equation 1 equal to each other, we obtain the quasi-stationary supersaturation within the cloud parcel: where A is a parameter depending on G , Q_1 and Q_2 (see Appendix).

Combining Equations 3, ?? and the definition of liquid water mixing ratio q_l for monodisperse droplets, we can get the linear growth rate of q_l . When supersaturation transients are negligible, e.g., after droplet activation, Equation 1 leads to linear growth rate of q_l ,

$$\frac{dq_l}{dt} = C_1 w, \quad (2)$$

where $C_1 = Q_1/Q_2$ with the units of m^{-1} (see Appendix). **This is the quasi-steady limit, in which the supersaturation is**

$$s_{qs} = \frac{Aw}{r_d n_d}, \quad (3)$$

where A is a parameter depending on G , Q_1 and Q_2 (see Appendix). If we assume C_1 is a constant, then q_l can be derived by integration of Equation 2,

$$q_l = C_1 z + q_{l,i}, \quad (4)$$

where $q_{l,i}$ is the initial liquid water mixing ratio, and $z = \int w dt$ is the displacement of the cloud parcel away from its initial location. The liquid water mixing ratio increases linearly with height and does not depend on the updraft velocity. It should be mentioned that Equation 4 describes q_l under thermodynamic equilibrium conditions. In reality, a cloud system needs some time (phase relaxation time) to reach the equilibrium state; For liquid clouds the phase relaxation time is usually smaller than 10 s (Korolev and Mazin, 2003).

During the adiabatic process, two physical properties of the cloud parcel will be conserved: total water mass mixing ratio and liquid water potential temperature (Kumar et al., 2014), such that

$$q_{l,i} + q_{v,i} = q_{l,f} + q_{v,f} \quad (5)$$

and

$$T_i - \frac{l_w}{c_p} q_{l,i} = T_f - \frac{l_w}{c_p} q_{l,f} \quad (6)$$

where q is the water mass mixing ratio (g/g), T is temperature (K), l_w is the latent heat of liquid water (J kg⁻¹) and c_p is the specific heat of air at constant pressure (J kg⁻¹K⁻¹). Subscripts l and v represent liquid and water vapor, respectively, while subscripts i and f denote the initial and final states of the cloud parcel. **It should be mentioned that we did not consider the pressure dependence of the liquid water potential temperature, which is valid if the cloud thickness is not too large.** We note that, for simplicity, the linearized form of the liquid water potential temperature has been used in Equation 6.

2.2 Liquid water mixing ratio in an adiabatic cloud after mixing

Now we consider the mixing of a cloud with dry and clean (aerosol free) environmental air and subsequent evolution for a closed, rising parcel. We define the mixing fraction as χ , such that χ fraction of cloud air is mixed with $(1 - \chi)$ fraction of environmental air. We assume the mixing process is isobaric, and that the time scale for the mixing is much smaller than the time scale for the response of the cloud droplets during the mixing (i.e., homogeneous mixing limit). Therefore after isobaric mixing but before any phase changes, the liquid water mixing ratio should be $\chi q_{l,i}$ and the water vapor mixing ratio should be $\chi q_{v,i} + (1 - \chi) q_{v,e}$ and the temperature of the mixed parcel should be $\chi T_i + (1 - \chi) T_e$. The subscript im represents the initial state of mixed parcel (before the evaporation of cloud droplets in the mixed parcel) and Subscript e denotes the state of

the environmental air. After the mixing, we assume the mixed parcel rises adiabatically again with a constant updraft velocity w_m . For the purposes of this derivation w_m is prescribed and we do not consider the actual buoyancy of the mixed parcel with respect to the environment. Similar to
 165 Equation 5 and 6, we have two conservation equations that allow the liquid water mixing ratio and temperature to be determined for the final state of the mixed parcel (Kumar et al., 2014), denoted by subscript fm :

$$\chi(q_{l,i} + q_{v,i}) + (1 - \chi)q_{v,e} = q_{l,fm} + q_{v,fm} \quad (7)$$

and

$$170 \quad \chi T_i + (1 - \chi)T_e - \frac{l_w \chi}{c_p} q_{l,i} = T_{fm} - \frac{l_w}{c_p} q_{l,fm}. \quad (8)$$

Now we ask, how does the liquid water mixing ratio in the mixed parcel ($q_{l,fm}$) change with height above the mixing level? What is the difference of liquid water mixing ratio in the mixing
 175 parcel ($q_{l,fm}$) compared with that in the original parcel without mixing ($q_{l,f}$) at the same height? How does the difference ($q_{l,f} - q_{l,fm}$) change with height? To calculate this difference, we first subtract Equation 7 from Equation 5 to get the liquid water difference for the final state,

$$q_{l,f} - q_{l,fm} = (1 - \chi)(q_{l,i} + q_{v,i} - q_{v,e}) - (q_{v,f} - q_{v,fm}). \quad (9)$$

The first term on the right side is the total water mixing ratio difference between the original and new
 180 parcel, which depends on the initial condition of the parcel ($q_{l,i}, q_{v,i}$), the environmental air ($q_{v,e}$), and the mixing fraction χ . This difference is large when χ is small and environmental air is dry. The second term on the right side is the water vapor mixing ratio difference. The water vapor mixing ratio can be calculated from temperature, pressure and saturation ratio: $q_v = \frac{S e_s(T) \epsilon}{p - e_s(T)}$. Therefore the difference of water vapor mixing ratio is

$$185 \quad q_{v,f} - q_{v,fm} = \frac{S_f e_s(T_f) \epsilon}{p_f - e_s(T_f)} - \frac{S_{fm} e_s(T_{fm}) \epsilon}{p_{fm} - e_s(T_{fm})}. \quad (10)$$

This equation is accurate but not simple enough to be useful. To achieve an analytical result, we first assume $p_f \approx p_{fm}$ because both parcels are at the same height. Secondly, we ignore e_s in the denominator because $p \gg e_s$. In addition, we assume both parcels are in quasi-steady state at that level and that the quasi-stationary supersaturation is much smaller than 1, so that the influence of the
 190 change of s_{qs} can be ignored compared with the change of $e_s(T)$ due to temperature; thus we assume $S_{fm} \approx S_f$. The main difference in the q_v arise from $e_s(T)$ due to the temperature differences. Using the linearized form of the Clausius-Clapeyron equation, we can approximate the difference of $e_s(T)$ as

$$e_s(T_f) - e_s(T_{fm}) \approx \frac{e_s(T_f) l_w}{p_f R T_f^2} (T_f - T_{fm}). \quad (11)$$

195 From the above assumptions and Equation 11, we can simplify Equation 10,

$$q_{v,f} - q_{v,fm} \approx \frac{S_f e_s(T_f) l_w \epsilon}{p_f R T_f^2} (T_f - T_{fm}). \quad (12)$$

Combining Equations 9 and 12, we find that the liquid water mixing ratio difference depends on the temperature difference in this way,

$$q_{l,f} - q_{l,fm} = (1 - \chi)(q_{l,i} + q_{v,i} - q_{v,e}) - \frac{S_f e_s(T_f) l_w \epsilon}{R T_f^2} (T_f - T_{fm}). \quad (13)$$

200 In addition, the difference in liquid water potential temperature conservation equations for closed and mixed parcels given by Equation 6 minus Equation 8, leads to

$$(1 - \chi)(T_i - T_e - \frac{l_w}{c_p \epsilon} q_{l,i}) = T_f - T_{fm} - \frac{l_w}{c_p \epsilon} (q_{l,f} - q_{l,fm}). \quad (14)$$

Finally, from Equations 13 and 14, we can obtain the approximate solutions for liquid water mixing ratio difference and temperature difference,

$$205 \quad q_{l,f} - q_{l,fm} = (1 - \chi) \frac{(1 + C_3)q_{l,i} + q_{v,i} - q_{v,e} - C_2(T_i - T_e)}{1 + C_3} \quad (15)$$

and

$$T_f - T_{fm} = (1 - \chi) \frac{C_2(T_i - T_e) + C_3(q_{v,i} - q_{v,e})}{C_2(1 + C_3)}. \quad (16)$$

Finally, combining Equations 4 and 15, we can get the liquid water profile for the mixed parcel,

$$q_{l,fm}(z) = C_1 z + q_{l,i} - (1 - \chi)K_1, \quad (17)$$

210 where $K_1 = ((1 + C_3)q_{l,i} + q_{v,i} - q_{v,e} - C_2(T_i - T_e))/(1 + C_3)$. It is interesting to see that the liquid water mixing ratio for the mixed parcel still increases linearly with height, but with a smaller value compared with an unmixed parcel (cf. Equation 4). The difference is the same at different heights, and is proportional to $1 - \chi$.

215 2.2.1 Total evaporation and reactivation height

Another way to look at Equation 17 is that the liquid water mixing ratio in the mixing parcel $q_{l,fm}$ increases with height linearly with the same slope as $q_{l,f}$ in the original parcel, but with a smaller initial liquid water mixing ratio in the mixing parcel $q_{l,im} = q_{l,i} - (1 - \chi)K_1$. Although the initial liquid water mixing ratio $q_{l,im}$ should be non-negative physically, $q_{l,i} - (1 - \chi)K_1$ can be negative mathematically. If $q_{l,im}$ is negative, it means that all cloud droplets evaporate. Therefore, $q_{l,i} = (1 - \chi)K_1$ is the criteria for critical condition that all droplets totally evaporate and the air in mixing parcel is just saturated. It is not difficult to prove that this critical condition is consistent with that given by Pinsky et al. (2015b), with $\gamma = 0$.

220

225 Even if $q_{l,fm}$ is negative at $z = 0$, it can become positive at higher altitude. The negative value of $q_{l,fm}$ at the beginning is the result of total evaporation, while the point where $q_{l,fm}$ changes to positive can be taken to represent the re-activation of cloud condensation nuclei to form cloud droplets. The re-activation height z_{react} is the distance between the mixing level and the level at which $q_{l,fm} = 0$, given by

$$230 \quad z_{react} = \frac{(1 - \chi)K_1 - q_{l,i}}{C_1}. \quad (18)$$

2.2.2 Critical height for superadiabatic droplet growth

In this subsection we consider how cloud droplet size changes with height above the mixing level. We consider an initially-adiabatic cloud parcel mixed isobarically with clean environmental air at some level above the cloud base. Without vertical movement, the liquid water mixing ratio and cloud number concentration will decrease due to dilution (not considering, for the moment, scenarios in which all droplets are evaporated). The mean cloud droplet size after the response to mixing is the same for extremely inhomogeneous mixing, but smaller for homogeneous mixing. If the parcel still rises adiabatically after mixing, however, the liquid water mixing ratio will increase with height (cf. Equation 17). This indicates that cloud droplet size will also increase with height, because the number concentration does not change during the vertical motion. We now consider the growth of cloud droplets under quasi-steady conditions. Because the cloud droplet concentration is smaller in the mixed parcel than in the original parcel, s_{qs} in the mixed parcel will be larger ($s_{qs} \propto (r_d n_d)^{-1}$, see Equation 3). This implies that cloud droplets in the mixing parcel grow faster than those in the original one due to higher supersaturation. This suggests that although cloud droplet size in the mixed parcel is smaller for homogeneous mixing at the beginning, it might, with adequate vertical displacement, become equal to or even larger than that in the original, unmixed parcel. The resulting droplets would appear to have experienced super-adiabatic growth compared to a closed parcel. This general picture of large-drop production resulting from decreased competition in diluted parcels has been discussed elsewhere in the literature (Paluch and Knight, 1986; Cooper et al., 2013; Schmeissner et al., 2015).

For a clean environment and homogeneous, it's true that $n_{d,fm}/n_{d,f} = \chi$ as long as droplets in the mixing parcel don't totally evaporate. Here n_d is the cloud droplet number concentration. For monodisperse cloud droplets if $q_{l,fm}/q_{l,f}$ also equals χ , it means that the droplet sizes in both mixing and original parcels are the same (because $q_l = 4/3\pi\rho_l r_d^3 N_d$). We define the critical height z^* as the height when droplets in both parcels have the same sizes. Based on the definition of liquid water mixing ratio, it is apparent that $q_{l,fm}/q_{l,f} = \chi$ at the critical height, and

260 therefore

$$\frac{C_1 z^* + q_{l,i} - (1 - \chi)K_1}{C_1 z^* + q_{l,i}} = \chi. \quad (19)$$

Solving Equation 19, we obtain

$$z^* = \frac{K_1 - q_{l,i}}{C_1}. \quad (20)$$

We note with interest that z^* is independent of the mixing fraction χ . Equations 17 and 20 indicate
265 that although the liquid water mixing ratio for the mixed parcel is always lower than that in the original parcel, droplet radius in the mixed parcel will be larger than that in the original parcel when the parcel is above z^* .

3 Results from parcel model

270 The analytical results derived in Section 2 have provided insight into the evolution of a cloud parcel after a mixing event, but several assumptions and simplifications were made, and some limitations such as perfectly clean (aerosol free) environment were imposed. We now explore the same concept of idealized mixing and subsequent-growth, but using an adiabatic parcel model with bin microphysics. The model was originally developed by Feingold et al. (1998) to simulate warm cloud
275 process and has been applied to a wide range of microphysical problems (Feingold and Kreidenweis, 2000; Xue and Feingold, 2004; Ervens et al., 2005; Ervens and Feingold, 2012; Yang et al., 2012; Li et al., 2013). To study the mixing process, we add an idealized entrainment/detrainment and mixing process to the model. Entrainment means some fraction of environment air flows into the cloud, while detrainment means some fraction of cloud flows into the environment (de Rooy et al., 2013).
280 The mixing process is implemented so that the entrained environmental air is homogeneously mixed with the remaining cloud body, and in all cases considered here this mixing level is set to 665 m (50 m above cloud base). It should be mentioned that mixing process might not necessarily happen when entrainment/detrainment occurs. The time interval between these two processes is called the mixing time scale, and the presence of a delay would be expected for inhomogeneous mixing. The relative
285 magnitudes of this mixing time scale and the phase relaxation time determine whether the mixing occurs in the homogeneous or inhomogeneous limit (e.g., Baker et al., 1980). To be consistent with the previous theoretical development (Sec. 2) we implement the homogeneous mixing limit within the model, i.e., the instantaneous exposure of droplets to the mixture of cloudy and entrained air. This implies that the turbulent mixing time is very small compared to the phase relaxation time, and
290 is therefore similar to the limit considered by Pinsky et al. (2015b).

Initial conditions for the parcel are $z_0 = 300$ m, $p_0 = 919$ Pa, $T_0 = 288.15$ K and $RH_0 = 85\%$. Cloud condensation nuclei (CCN) are ammonium sulfate particles with a monodisperse radius of

50 nm and concentration of 50 mg^{-1} . The parcel rises adiabatically with constant updraft velocity.
295 Two updraft velocities (w) are chosen in this study: 0.1 and 1.0 m s^{-1} . Observation results show that updraft velocity in cumulus cloud is on the order of 1.0 m s^{-1} , and that for stratocumulus cloud is on the order of 0.1 m s^{-1} (Katzwinkel et al., 2014a; Ditas et al., 2012). Cloud base is reached at $z = 615 \text{ m}$, where CCN are activated as cloud droplets. The isobaric mixing process occurs at $z = 665 \text{ m}$, 50 m above the cloud base. For simplicity, we assume the environmental temperature at
300 the mixing level is the same as that of the cloud parcel, but the relative humidity is only 85%. After the mixing, the new mixed parcel rises adiabatically again with the same updraft velocity.

Liquid water mixing ratio profiles for six different mixing fractions $\chi = 1.0, 0.9, 0.8, 0.7, 0.6, 0.5$ at $w = 0.1 \text{ m s}^{-1}$ are shown in Figure 1 (a). The analytical results based on Equation 17 are also
305 shown and are quite close to the results from the parcel model. As seen from Figure 1 (a), the liquid water mixing ratio for smaller χ is smaller than that for larger χ at the same height. In addition, when $\chi \leq 0.8$, the liquid water mixing ratio will decrease to zero at the beginning, which means that the cloud totally evaporates and becomes subsaturated. It should be mentioned that in the model each cloud droplet contains one CCN, and when a cloud droplet totally evaporates the CCN still survives.
310 Because the subsaturated parcel still rises adiabatically, CCN in the mixing parcel can be activated again when the air becomes saturated at a higher level, which we defined as the re-activation level. The smaller χ is, the higher the re-activation level is. The evaporation and re-activation processes can be clearly seen from the cloud droplet radius profile in Figure 1 (b). In addition, it clearly shows that the mixed cloud parcel can reach super-adiabatic growth conditions (where the cloud droplet radius
315 in the mixed parcel is larger than that in the original, unmixed parcel with $\chi = 1.0$) above a critical height. The critical height is independent of χ and agrees well with that predicted by Equation 20. **The saturation ratio and cloud droplet number concentration profiles for this case are shown in Figure S1 (supplementary material). It can be seen that cloud droplet number concentration in the mixed parcel decreases with decreasing χ , while supersaturation increases with decreasing χ in the quasi-steady region.**
320

Results above are for a cloud parcel mixing with clean environmental air (aerosol free condition). However, both observational and modeling results show that air around the cumulus cloud is usually not clean (Katzwinkel et al., 2014a; Chen et al., 2012). There can be background aerosols in the at-
325 mosphere even at high altitude, and in addition, subsiding shells can also provide sufficient aerosols as CCN when mixing occurs (Heus and Jonker, 2008). There is no simple analytical result for mixing with a polluted environment. However, we can use the parcel model to investigate the effect of mixing when the environmental air is polluted. For simplicity, we assume the environment has the same dry aerosol size distribution as that below the cloud base.

330

Figure 1 (c) shows the monodisperse cloud droplet radius versus height for various χ after mixing with a polluted environment at $w = 0.1 \text{ m s}^{-1}$. For $\chi = 0.9$, the remaining cloud droplets do not totally evaporate and the entrained aerosols are not activated as cloud droplets. For smaller χ , the remaining cloud droplets totally evaporate and leave CCN in the mixed parcel. Both entrained and remaining CCN are activated at a higher level. In addition, only the parcel with $\chi = 0.9$ can reach the super-adiabatic growth region. For smaller χ , cloud droplets are smaller than those in the original parcel at the same height z^* . ~~This is similar to the aerosol indirect effect in which more aerosols leads to smaller cloud droplets.~~ In summary, when mixing with a polluted environment, the mixing parcel can reach super-adiabatic growth conditions at the predicted z^* only if the cloud does not totally evaporate after mixing. **Saturation ratio and cloud droplet concentration profiles for various mixing fractions are shown in Figure S2. Supersaturation in the quasi-steady state is smaller than that when mixing with the clean environmental air as shown in Figure S1. This is because the entrained aerosols from the polluted environmental air can be activated as cloud droplets and thus suppress the supersaturation in the mixed parcel.**

Figure 2 (a) and (b) show the results for mixing with a clean environment at larger updraft velocity $w = 1.0 \text{ m s}^{-1}$. It can be seen that the liquid water mixing ratio and cloud droplet radius profiles are almost the same compared with Figure 1, except that the mixing parcel totally evaporate for $\chi = 0.8$ at $w = 0.1 \text{ m s}^{-1}$, but doesn't totally evaporate for $\chi = 0.8$ at $w = 1.0 \text{ m s}^{-1}$. This is because larger updraft velocity supplies more water within the fixed phase relaxation time, so droplets begin to grow before they have had time to completely evaporate. The mixed parcel can reach the super-adiabatic growth region when it is above z^* . And as before, z^* is independent of both mixing fraction and updraft velocity, consistent with the theoretical prediction.

When mixing with polluted environment air at $w = 1.0 \text{ m s}^{-1}$, the mixed parcel can't reach the super-adiabatic growth region whether the mixing parcel totally evaporates or not (see Figure 2 (c)). The reason is that with large updraft velocity, the entrained CCN can always be activated as cloud droplets, thus compete for water vapor in the mixed parcel. It should be mentioned that results here strongly depend on the physical and chemical properties of the entrained CCN, e.g., sizes, chemical composition, and number concentration. For example, the mixed parcel might also reach the super-adiabatic growth region if the environmental air only contains a small number of CCN. In general, however, mixing with polluted air will inhibit the super-adiabatic growth of cloud droplets. **Saturation ratio and cloud droplet number concentration profiles for clean and polluted conditions with high updraft velocity are shown in Figure S3 and S4 separately.**

Cloud droplets in a real cloud are usually polydisperse and we now consider to what extent the theoretical predictions apply in this more complex system. The effect of mixing on a polydisperse

droplet population is tested with the cloud parcel model. The initial aerosols are composed of ammonium sulfate and are distributed lognormally in 20 bins with 50 nm median radius, standard deviation of 1.4, and a total number concentration of 100 cm^{-3} . Initial radii of the dry aerosols for the 20 bins are listed in **the supplementary material Table ??**. The cloud droplet diameters for each bin versus height for $\chi = 0.9, 0.7, 0.5$ are shown in Figure 3. These results are for clean environmental air and $w = 0.1 \text{ m s}^{-1}$ and are representative of the other cases. It can be seen that not all 20 bins are activated at cloud base; for example, only the largest 11 aerosol sizes are activated as cloud droplets for $\chi = 1.0$. Cloud droplets evaporate a little bit for $\chi = 0.9$, or completely for $\chi = 0.7, 0.5$, and re-activation occurs again at a higher level. It is very interesting to see that for $\chi = 0.5$, the 12th bin is not activated at cloud base, but is activated for the first time after mixing (green line). This asymmetric phenomenon is due to the significant reduction of cloud droplet number concentration after mixing. Thermodynamic equilibrium predicts how much water vapor should condense at a certain level, but mixing with a clean environment reduces the overall CCN concentration. To condense the same amount of water, either the single droplets must grow larger than before, which is the physical explanation for super-adiabatic growth; or some initially un-activated aerosol particles can be activated to increase the cloud number concentration.

Super-adiabatic droplet growth for individual droplet size bins can be observed in Figure 3, but it is achieved at different heights above the mixing level. Figure 4 shows these critical heights for individual cloud droplet size bins calculated from the cloud parcel model for the various mixing fractions. Here again, the environmental air is clean with $T_e = T_c$ and $RH_e = 85\%$. We note that cloud droplet size decreases with increasing bin number (i.e., cloud droplet size increases with increasing dry aerosol size, as expected). The critical height for each bin is defined when the sizes of cloud droplets for that bin are equal for both mixed and unmixed cloud parcels. It can be seen that the critical height depends on the size of the cloud droplet, the mixing fraction and the updraft velocity, especially for low updraft velocity $w = 0.1 \text{ m s}^{-1}$. For $w = 1.0 \text{ m s}^{-1}$, critical heights for individual bins are close to the theoretical critical height for a monodisperse cloud droplet population. In the low updraft speed case (left panel) it is particularly striking that the $\chi = 0.9$ curve has a different dependence than that for the other mixing fractions: increasing rather than decreasing z^* with decreasing droplet size. We believe the explanation is that the $\chi = 0.9$ case is the only scenario in which complete droplet evaporation does not occur. Thus, the presence of complete evaporation and subsequent re-activation changes the population dynamics of the cloud substantially for low updraft speeds. Although the critical heights are different for individual size bins, we might expect that the simple monodisperse prediction for z^* would hold for some moment of cloud droplet size distribution. Considering that the thermodynamically-predicted water mass is distributed over a variable number of aerosol particles, the most logical choice is a prediction of z^* using the volume-mean radius. Figure 5 shows the volume-weighted mean radius as a function of height for six values of χ

405 and for updraft speeds of 0.1 and 1.0 m s⁻¹. In spite of the complex behavior observed for individual bins, the volume-mean radius curves are observed to cross at nearly the same height and with very close agreement with the analytical prediction. This suggests that the theory can be applied under realistic cloud conditions with polydisperse droplet populations. **Figures S5 and S6 show the saturation ratio and cloud droplet number concentration profiles for polydisperse cloud droplets**
410 **at low and high updraft velocity separately. Our results are similar to Wang et al. (2009), where they observed faster droplet growth resulting from reduced droplet number concentration and increased supersaturation in a mixed parcel.**

4 Discussion and conclusions

415 In this study, we have considered isobaric mixing of a cloud parcel with environmental air, and then the subsequent droplet growth as the parcel rises adiabatically afterwards. Analytical expressions are derived for monodisperse cloud droplets when mixing with clean environmental air. Results show that the liquid water mixing ratio q_l in the mixed parcel increases linearly with height with the same slope ($\frac{dq_l}{dz}$) as the original parcel (without mixing). Due to the mixing the q_l is smaller compared with
420 the unmixed parcel at the same height. A closed form expression for the offset is derived and shows that the decrease of q_l in the mixed parcel depends on the mixing fraction χ and the temperature and relative humidity of the environmental air. A critical height z^* , defined as the height at which the cloud droplet sizes are equal in both mixed and original cloud parcels, is derived. Interestingly, the critical height depends on the initial conditions of the cloud and environmental air, but is inde-
425 pendent of the mixing fraction. Cloud droplets in the mixed parcel are larger than in the original parcel above z^* , which we call the “super-adiabatic” growth region. These large cloud droplets may help explain the formation of initial large droplets that contribute to precipitation formation in warm clouds.

430 The predicted vertical profile of liquid water mixing ratio and the critical height are confirmed using a bin microphysical cloud model. For large χ and a humid environment, cloud droplets will evaporate a little bit and grow again after mixing. For small χ and dry environment, cloud droplets can evaporate completely, leaving the mixed parcel subsaturated. Droplets are re-activated at a higher level, as long as the mixing parcel rises sufficiently to reach saturation again. The theoretical predic-
435 tions are based on equilibrium arguments, but because the phase relaxation time is typically short for warm clouds, results are not very sensitive to updraft speed over the range investigated. For monodisperse cloud droplets, z^* is independent of mixing fraction and updraft speed. For polydisperse cloud droplets, however, z^* defined for individual droplet sizes is observed to depend on droplet size, mixing fraction and updraft velocity, especially for smaller w . For larger w , z^* is insensitive to those

440 variables and close to the analytical result for monodisperse cloud droplets. The situation becomes much simpler and the polydisperse cloud can be predicted theoretically by using the volume-mean cloud droplet radius. Finally, we note that the model results presented here are for the condition of cloud and environment having the same temperature; model runs for other reasonable conditions also produced good agreement with the theory.

445

Environment background aerosols and subsiding shells may contain effective CCN that can be activated after mixing, thus inhibiting super-adiabatic droplet growth. For large updraft speed, the entrained aerosols can be activated as cloud droplets, thus increasing cloud droplet concentration and decreasing the cloud droplet sizes. For small updraft velocity, the mixed parcel can reach the super-adiabatic growth region only when the entrained aerosols cannot be activated and the cloud droplets do not totally evaporate. Otherwise if cloud droplets totally evaporate, both remaining and entrained CCN can be activated when the mixed parcel is saturated again. If the entrained aerosols can be activated as cloud droplets, the mixed parcel usually contains smaller cloud droplets, but similar number concentration compared with the main cloud body. This might help explain the observation that some cloud samples appear to be undiluted in droplet number concentration, but have significantly smaller mean-volume radii, a region otherwise outside the homogeneous mixing limiting curve in a mixing diagram (Schmeissner et al., 2015).

Given the success of the analytical results in predicting the critical height z^* above which volume-weighted mean droplet diameters will appear to be super-adiabatic, we briefly explore the dependence of z^* on environmental conditions. As noted already, and now confirmed by the parcel model, the critical height does not depend on mixing fraction χ or on the updraft speed w . As seen in Figure 6, z^* changes with the relative humidity of the environmental air (RH_e) at the mixing level. It can be seen that z^* decreases as RH_e increases. For example, when $RH_e = 98\%$, z^* is less than 50 m above the mixing level. This means that the mixed parcel can reach the super-adiabatic growth region more easily when mixing with a humid environment. **Thus the results are relevant to shallow convective clouds, in contrast with the particular example chosen for Figures 1-5 that requires a height of approximately 300 m above the mixing level for super-adiabatic growth.** In the real atmosphere, **this has relevance for at least two scenarios. First, for cumulus convection** the subsiding shell ~~around a cumulus cloud in a clean environment might~~ can be very humid due to the evaporation of cloud droplets at higher cloud levels (**Katzwinkel et al., 2014b**). Mixing under these conditions would be favorable for super-adiabatic growth of cloud droplets, especially if the subsiding shell has been cleared of most CCN through scavenging. **Second, for stratocumulus convection the concepts here can hold for mixing between undiluted cloud parcels and parcels previously diluted through cloud-top mixing (followed by descent together with cloud droplet evaporation and humidification).** Upon subsequent lifting after mixing with the diluted but humid parcel,

475

super-adiabatic droplets can be produced, in analogy with the mechanism described by Wang et al. (2009)

480 The results presented here all are for the homogeneous mixing limit. It is possible to develop model prescriptions for extreme inhomogeneous mixing, but our sense is that the results would be sensitive to the necessarily artificial nature of those prescriptions. Ultimately, a realistic model or a direct numerical simulation of the mixing process are required for the inhomogeneous limit. We can speculate, however, that the results obtained here would only be amplified for inhomogeneous
485 mixing: in that limit the droplet concentration is reduced but the mean volume diameter remains unchanged, implying that z^* is zero and super-adiabatic droplet growth can begin immediately after the mixing process has concluded. By concluded we mean that the cloudy and environmental air have become completely mixed, leaving a spatially homogeneous field of droplets having the same diameter as before mixing, but lower number concentration due to dilution and total evaporation of
490 some subset of droplets (e.g., Beals et al., 2015). This neglects the more complicated interactions that might come into play if CCN are entrained during mixing with environmental air: in that case activation of new CCN may occur as the parcel rises, even before complete mixing to the microscale has taken place.

A crucial factor that has not been considered thus far is the influence of mixing on the vertical motion of a cloud parcel due to changes in its buoyancy. Whether a mixed cloud parcel can experience
495 super-adiabatic droplet growth depends not only on the critical height z^* , but also on the maximum height z_{max} it can reach after mixing: a cloud can reach the super-adiabtic growth region only for $z_{max} > z^*$. Calculation of z_{max} is nontrivial because one must consider the time dependence of the buoyancy, drag force, and kinetic energy of the parcel, which depends on the properties of the
500 surrounding environment and and its dependence on height. These are still open research problems (e.g., slippery versus sticky thermals (Sherwood et al., 2013; Romps and Charn, 2015)), so exploring this important aspect is beyond the scope of our paper; but qualitatively, our results imply that strongly convective clouds may favor super-adiabatic growth compared to weakly convective clouds. In addition, decreasing χ will tend to decrease the buoyancy and therefore the updraft speed, thus
505 ultimately decreasing z_{max} . Therefore, it is more likely to reach the super-adiabatic droplet growth region for larger χ , again favoring clouds in humid environments or clouds with well developed, humid subsiding shells.

In a real cloud the liquid water mixing ratio profile is much more complicated than considered
510 here. Mixing will occur at different levels and environmental conditions change with height. There are several methods to predict the mixing fraction at different levels. For example, Lu et al. (2012) predict χ using the cloud base condition, liquid water mixing ratio and environmental condition at each level. The advantage of their method is that they do not need to measure temperature and water

vapor mixing ratio in the cloud, which have significant measurement uncertainty. Here, we have provided an explicit method to estimate the mixing fraction at each level using a similar strategy. Based on Equation 15 and 16, we can also calculate the mixing fraction profile. The key difference is that our method is explicit, while their method is implicit.

The central insights of this work are **the derived height for super-adiabatic growth and the findings** that a mixed parcel is more likely to reach the super-adiabatic growth region when convection is strong, and the environmental air is humid and clean. Cloud droplets in the super-adiabatic growth region are larger than that in an unmixed parcel. The theoretical results obtained here and confirmed with the parcel model is a step toward evaluating the possible role of mixing-induced droplet growth for large droplet production and development of precipitation in warm clouds.

Acknowledgements. This research was supported by the DOE Office of Science as part of the Atmospheric System Research program through Grant No. DE-SC0011690.

Appendix A: List of Symbols

Table 1. List of Symbols

Symbol	Description	Units
A	$\frac{Q_1}{4\pi\rho_w G Q_2}$	s kg^{-1}
c_p	specific heat of air at constant temperature	$\text{J kg}^{-1} \text{K}^{-1}$
C_1	$4\pi\rho_w G A = Q_1/Q_2$	m^{-1}
C_2	$\frac{S_f e_s(T_f) l_w \epsilon}{p_f R_v T_f^2}$	K^{-1}
C_3	$\frac{C_2 l_w}{\epsilon_p}$	—
D_v	Diffusivity of water vapor	$\text{m}^2 \text{s}^{-1}$
e_v	water vapor pressure	Pa
$e_s(T)$	saturated water vapor pressure at temperature T	Pa
G	$\left[\frac{\rho_w R_v T}{D_v e_s(T)} + \frac{\rho_w l_w}{k_T T} \left(\frac{l_w}{R_v T} - 1 \right) S \right]^{-1}$	$\text{m}^2 \text{s}^{-1}$
k_T	coefficient of air heat conductivity	$\text{J m}^{-1} \text{s}^{-1}$
K_1	$\frac{(1+C_3)q_{l,i}+q_{v,i}-q_{v,e}-C_2(T_i-T_e)}{1+C_3}$	—
K_2	$\frac{C_2(T_i-T_e)+C_3(q_{v,i}-q_{v,e})}{C_2(1+C_3)}$	K
l_w	latent heat of liquid water	J kg^{-1}
M_{air}	molar mass of air	kg mol^{-1}
M_w	molar mass of water	kg mol^{-1}
n_d	droplet number per unit mass of air	kg^{-1}
q_l	liquid water mixing ratio	—
$q_{l,i}$	initial q_l	—
$q_{l,f}$	final q_l	—
q_v	water vapor mixing ratio	—
$q_{v,e}$	environmental q_v	—
$q_{v,i}$	initial q_v	—
$q_{v,f}$	final q_v	—
Q_1	$\frac{q l_w}{c_p R_v T^2} - \frac{q}{R_a T}$	m^{-1}
Q_2	$\frac{\rho_{air} l_w^2}{p c_p T} + \frac{\rho_{air} R_v T}{e_s(T)}$	—
r_d	radius of cloud droplet	m
$r_{d,i}$	initial r_d	m
$r_{d,f}$	final r_d	m
$r_{d,fm}$	final r_d with mixing fraction χ	m
R	universal gas constant	$\text{J mol}^{-1} \text{K}^{-1}$
R_a	gas constant for dry air	$\text{J kg}^{-1} \text{K}^{-1}$
R_v	gas constant for water vapor	$\text{J kg}^{-1} \text{K}^{-1}$
s	$S - 1$, water vapor supersaturation	—
S	$\frac{e_v}{e_s}$, water vapor saturation ratio	—
S_f	final S	—
S_{fm}	final S with mixing fraction χ	—
T	temperature	K
T_i	initial T	K
T_{im}	initial T with mixing fraction χ	K
T_e	environmental T	K
T_f	final T	K
T_{fm}	final T with mixing fraction χ	K
w	updraft velocity of cloud parcel	m s^{-1}
w_m	updraft velocity of cloud parcel with mixing fraction χ	m s^{-1}
χ	isobaric mixing fraction	—
ϵ	$\frac{M_w}{M_{air}}$	—
κ	$\frac{R}{c_p}$	—
ρ_w	density of liquid water	kg m^{-3}
ρ_{air}	density of air	kg m^{-3}

References

- 530 Andrejczuk, M., Grabowski, W. W., Malinowski, S. P., and Smolarkiewicz, P. K.: Numerical simulation of cloud-clear air interfacial mixing: Effects on cloud microphysics, *Journal of the atmospheric sciences*, 63, 3204–3225, 2006.
- Andrejczuk, M., Grabowski, W. W., Malinowski, S. P., and Smolarkiewicz, P. K.: Numerical simulation of cloud-clear air interfacial mixing: homogeneous versus inhomogeneous mixing, *Journal of the Atmospheric Sciences*, 66, 2493–2500, 2009.
- 535 Baker, M., Corbin, R., and Latham, J.: The influence of entrainment on the evolution of cloud droplet spectra: I. A model of inhomogeneous mixing, *Quarterly Journal of the Royal Meteorological Society*, 106, 581–598, 1980.
- Beals, M. J., Fugal, J. P., Shaw, R. A., Lu, J., Spuler, S. M., and Stith, J. L.: Holographic measurements of inhomogeneous cloud mixing at the centimeter scale, *Science*, 350, 87–90, 2015.
- 540 Beard, K. V. and Ochs III, H. T.: Warm-rain initiation: An overview of microphysical mechanisms, *Journal of Applied Meteorology*, 32, 608–625, 1993.
- Blyth, A. M., Lasher-Trapp, S. G., Cooper, W. A., Knight, C. A., and Latham, J.: The role of giant and ultragiant nuclei in the formation of early radar echoes in warm cumulus clouds, *Journal of the atmospheric sciences*, 60, 2557–2572, 2003.
- 545 Burnet, F. and Brenguier, J.-L.: Observational study of the entrainment-mixing process in warm convective clouds, *Journal of the atmospheric sciences*, 64, 1995–2011, 2007.
- Chen, G., Xue, H., Feingold, G., and Zhou, X.: Vertical transport of pollutants by shallow cumuli from large eddy simulations, *Atmospheric Chemistry and Physics*, 12, 11 319–11 327, 2012.
- Chen, J., Liu, Y., and Zhang, M.: Investigation the influences of entrainment mixing processes on cloud micro-
550 physics using new cloud parcel model, AGU Fall Meeting, 2015.
- Cheng, W. Y., Carrió, G. G., Cotton, W. R., and Saleeby, S. M.: Influence of cloud condensation and giant cloud condensation nuclei on the development of precipitating trade wind cumuli in a large eddy simulation, *Journal of Geophysical Research: Atmospheres (1984–2012)*, 114, 2009.
- Cooper, W. A., Lasher-Trapp, S. G., and Blyth, A. M.: The influence of entrainment and mixing on the initial
555 formation of rain in a warm cumulus cloud, *Journal of the Atmospheric Sciences*, 70, 1727–1743, 2013.
- Cotton, W. R., Bryan, G., and Van den Heever, S. C.: *Storm and cloud dynamics*, vol. 99, Academic press, 2011.
- de Rooy, W. C., Bechtold, P., Fröhlich, K., Hohenegger, C., Jonker, H., Mironov, D., Pier Siebesma, A., Teixeira, J., and Yano, J.-I.: Entrainment and detrainment in cumulus convection: an overview, *Quarterly Journal of the Royal Meteorological Society*, 139, 1–19, 2013.
- 560 Ditas, F., Shaw, R. A., Siebert, H., Simmel, M., Wehner, B., and Wiedensohler, A.: Aerosols-cloud microphysics-thermodynamics-turbulence: evaluating supersaturation in a marine stratocumulus cloud, *Atmospheric Chemistry and Physics*, 12, 2459–2468, 2012.
- Ervens, B. and Feingold, G.: On the representation of immersion and condensation freezing in cloud models using different nucleation schemes, *Atmospheric Chemistry and Physics*, 12, 5807–5826, 2012.
- 565 Ervens, B., Feingold, G., and Kreidenweis, S. M.: Influence of water-soluble organic carbon on cloud drop number concentration, *Journal of Geophysical Research: Atmospheres (1984–2012)*, 110, 2005.

- Feingold, G. and Kreidenweis, S.: Does cloud processing of aerosol enhance droplet concentrations?, *Journal of Geophysical Research: Atmospheres* (1984–2012), 105, 24 351–24 361, 2000.
- Feingold, G., Walko, R., Stevens, B., and Cotton, W.: Simulations of marine stratocumulus using a new micro-
570 physical parameterization scheme, *Atmospheric research*, 47, 505–528, 1998.
- Feingold, G., Cotton, W. R., Kreidenweis, S. M., and Davis, J. T.: The impact of giant cloud condensation nuclei on drizzle formation in stratocumulus: Implications for cloud radiative properties, *Journal of the atmospheric sciences*, 56, 4100–4117, 1999.
- Gerber, H., Frick, G., Jensen, J., and Hudson, J.: Entrainment, mixing, and microphysics in trade-wind cumulus,
575 *J. Meteor. Soc. Japan*, 86, 87–106, 2008.
- Göke, S., Ochs III, H. T., and Rauber, R. M.: Radar analysis of precipitation initiation in maritime versus continental clouds near the Florida coast: Inferences concerning the role of CCN and giant nuclei, *Journal of the Atmospheric Sciences*, 64, 3695–3707, 2007.
- Heus, T. and Jonker, H. J.: Subsiding shells around shallow cumulus clouds, *Journal of the Atmospheric Sci-
580 ences*, 65, 1003–1018, 2008.
- Hocking, L.: The collision efficiency of small drops, *Quarterly Journal of the Royal Meteorological Society*, 85, 44–50, 1959.
- Jensen, J., Austin, P., Baker, M., and Blyth, A.: Turbulent mixing, spectral evolution and dynamics in a warm cumulus cloud, *Journal of the atmospheric sciences*, 42, 173–192, 1985.
- 585 Jensen, J. B. and Lee, S.: Giant sea-salt aerosols and warm rain formation in marine stratocumulus, *Journal of the atmospheric sciences*, 65, 3678–3694, 2008.
- Johnson, D. B.: The role of giant and ultragiant aerosol particles in warm rain initiation, *Journal of the Atmospheric Sciences*, 39, 448–460, 1982.
- Katzwinkel, J., Siebert, H., Heus, T., and Shaw, R. A.: Measurements of turbulent mixing and subsiding shells
590 in trade wind cumuli, *Journal of the Atmospheric Sciences*, 71, 2810–2822, 2014a.
- Katzwinkel, J., Siebert, H., Heus, T., and Shaw, R. A.: Measurements of turbulent mixing and subsiding shells in trade wind cumuli, *Journal of the Atmospheric Sciences*, 71, 2810–2822, 2014b.
- Korolev, A., Pinsky, M., and Khain, A.: A New Mechanism of Droplet Size Distribution Broadening during Diffusional Growth, *Journal of the Atmospheric Sciences*, 70, 2051–2071, 2013.
- 595 Korolev, A., Khain, A., Pinsky, M., and J, F.: Theoretical analysis of mixing in liquid clouds–Part 1: Classical concept, *Atmospheric Chemistry and Physics Discussions*, 15, 30 211–30 267, 2015.
- Korolev, A. V. and Mazin, I. P.: Supersaturation of water vapor in clouds, *Journal of the atmospheric sciences*, 60, 2957–2974, 2003.
- Kostinski, A. B. and Shaw, R. A.: Fluctuations and luck in droplet growth by coalescence, *Bulletin of the
600 American Meteorological Society*, 86, 235–244, 2005.
- Kumar, B., Schumacher, J., and Shaw, R. A.: Lagrangian mixing dynamics at the cloudy-clear air interface, *Journal of the Atmospheric Sciences*, 2014.
- Laird, N. F., Ochs Iii, H. T., Rauber, R. M., and Miller, L. J.: Initial precipitation formation in warm Florida cumulus, *Journal of the atmospheric sciences*, 57, 3740–3751, 2000.
- 605 Lamb, D. and Verlinde, J.: *Physics and chemistry of clouds*, Cambridge University Press, 2011.

- Lasher-Trapp, S. G., Cooper, W. A., and Blyth, A. M.: Broadening of droplet size distributions from entrainment and mixing in a cumulus cloud, *Quarterly Journal of the Royal Meteorological Society*, 131, 195–220, 2005.
- Lehmann, K., Siebert, H., and Shaw, R. A.: Homogeneous and inhomogeneous mixing in cumulus clouds: dependence on local turbulence structure, *Journal of the Atmospheric Sciences*, 66, 3641–3659, 2009.
- 610 Li, Z., Xue, H., and Yang, F.: A modeling study of ice formation affected by aerosols, *Journal of Geophysical Research: Atmospheres*, 118, 11–213, 2013.
- Lozar, A. d. and Muessle, L.: Long-resident droplets at the stratocumulus top, *Atmospheric Chemistry and Physics Discussions*, 2016.
- Lu, C., Liu, Y., Yum, S. S., Niu, S., and Endo, S.: A new approach for estimating entrainment rate in cumulus
615 clouds, *Geophysical Research Letters*, 39, 2012.
- Lu, C., Niu, S., Liu, Y., and Vogelmann, A. M.: Empirical relationship between entrainment rate and microphysics in cumulus clouds, *Geophysical Research Letters*, 40, 2333–2338, 2013.
- Magaritz-Ronen, L., Pinsky, M., and Khain, A.: Effects of Turbulent Mixing on the Structure and Macroscopic Properties of Stratocumulus Clouds Demonstrated by a Lagrangian Trajectory Model, *Journal of the Atmospheric Sciences*, 71, 1843–1862, 2014.
620
- Magaritz-Ronen, L., Pinsky, M., and Khain, A.: Drizzle formation in stratocumulus clouds: effects of turbulent mixing, *Atmospheric Chemistry and Physics Discussions*, 15, 24 131–24 177, 2015.
- Naumann, A. K. and Seifert, A.: A Lagrangian drop model to study warm rain microphysical processes in a shallow cumulus, *Journal of Advances in Modeling Earth Systems*, 7, 1136–1154, 2015.
- 625 Paluch, I. R. and Knight, C. A.: Does mixing promote cloud droplet growth?, *Journal of the atmospheric sciences*, 43, 1994–1998, 1986.
- Pinsky, M., Khain, A., and Korolev, A.: Theoretical analysis of mixing in liquid clouds—Part 3: Inhomogeneous mixing, *Atmospheric Chemistry and Physics Discussions*, 15, 30 321–30 381, 2015a.
- Pinsky, M., Khain, A., Korolev, A., and L, M.-R.: Theoretical analysis of mixing in liquid clouds—Part 2: Homogeneous mixing, *Atmospheric Chemistry and Physics Discussions*, 15, 30 269–30 320, 2015b.
630
- Pruppacher, H. R., Klett, J. D., and Wang, P. K.: *Microphysics of clouds and precipitation*, Taylor & Francis, 1998.
- Romps, D. M. and Charn, A. B.: Sticky thermals: Evidence for a dominant balance between buoyancy and drag in cloud updrafts, *Journal of the Atmospheric Sciences*, 72, 2890–2901, 2015.
- 635 Schmeissner, T., Shaw, R., Ditas, J., Stratmann, F., Wendisch, M., and Siebert, H.: Turbulent Mixing in Shallow Trade Wind Cumuli: Dependence on Cloud Life Cycle, *Journal of the Atmospheric Sciences*, 72, 1447–1465, 2015.
- Sherwood, S. C., Hernández-Deckers, D., Colin, M., and Robinson, F.: Slippery Thermals and the Cumulus Entrainment Paradox*, *Journal of the Atmospheric Sciences*, 70, 2426–2442, 2013.
- 640 Su, C.-W., Krueger, S. K., McMurtry, P. A., and Austin, P. H.: Linear eddy modeling of droplet spectral evolution during entrainment and mixing in cumulus clouds, *Atmospheric research*, 47, 41–58, 1998.
- Tölle, M. H. and Krueger, S. K.: Effects of entrainment and mixing on droplet size distributions in warm cumulus clouds, *Journal of Advances in Modeling Earth Systems*, 6, 281–299, 2014.
- Wang, J., Daum, P. H., Yum, S. S., Liu, Y., Senum, G. I., Lu, M.-L., Seinfeld, J. H., and Jonsson, H.: Observations of marine stratocumulus microphysics and implications for processes controlling droplet spectra:
645

Results from the Marine Stratus/Stratocumulus Experiment, *Journal of Geophysical Research: Atmospheres*, 114, 2009.

Xue, H. and Feingold, G.: A modeling study of the effect of nitric acid on cloud properties, *Journal of Geophysical Research: Atmospheres* (1984–2012), 109, 2004.

650 Yang, F., Xue, H., Deng, Z., Zhao, C., and Zhang, Q.: A closure study of cloud condensation nuclei in the North China Plain using droplet kinetic condensational growth model, *Atmospheric Chemistry and Physics*, 12, 5399–5411, 2012.

Yin, Y., Levin, Z., Reisin, T. G., and Tzivion, S.: The effects of giant cloud condensation nuclei on the development of precipitation in convective clouds—A numerical study, *Atmospheric Research*, 53, 91–116,

655 2000.

Yum, S. S., Wang, J., Liu, Y., Senum, G., Springston, S., McGraw, R., and Yeom, J. M.: Cloud microphysical relationships and their implication on entrainment and mixing mechanism for the stratocumulus clouds measured during the VOCALS project, *Journal of Geophysical Research: Atmospheres*, 2015.

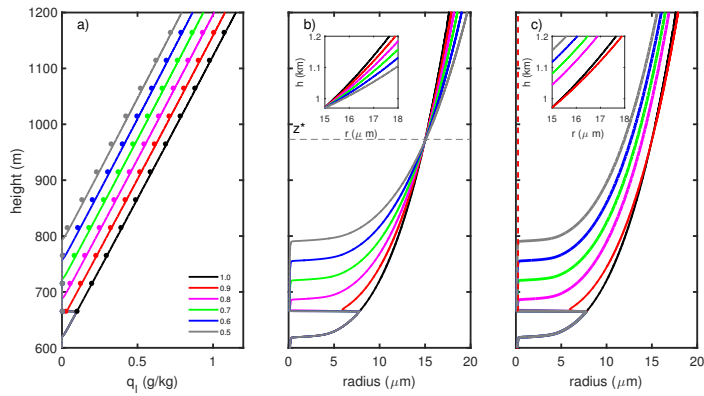


Figure 1. (a) Liquid water mixing ratio profiles for various cloud mixing fractions χ and with low updraft speed (0.1 m s^{-1}). Lines are from the parcel model and dots are from the theoretical prediction given by Equation 17. (b) Cloud droplet radius versus height for various χ when mixing with clean (aerosol free) environmental air. The horizontal dashed line represents the critical height z^* calculated from Equation 20. (c) Cloud droplet radius versus height for various χ when mixing with polluted environmental air (air containing CCN similar to cloud base conditions). Insets in (b) and (c) show details of the radius profiles above the critical height. Super-adiabatic droplet growth, i.e. droplet diameters greater than in the unmixed cloud ($\chi = 1.0$), is observed for all χ in (b) and only for $\chi = 0.9$ in (c).

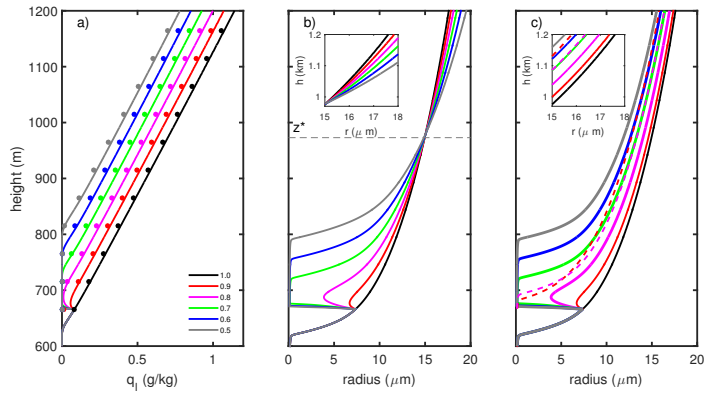


Figure 2. (a) Liquid water mixing ratio profiles for various cloud mixing fractions χ and with high updraft speed (1.0 m s^{-1}). Lines are from the parcel model and dots are from the theoretical prediction given by Equation 17. (b) Cloud droplet radius versus height for various χ when mixing with clean (aerosol free) environmental air. The horizontal dashed line represents the critical height z^* calculated from Equation 20. (c) Cloud droplet radius versus height for various χ when mixing with polluted environmental air (air containing CCN similar to cloud base conditions). Insets in (b) and (c) show details of the radius profiles above the critical height. Super-adiabatic droplet growth, i.e. droplet diameters greater than in the unmixed cloud ($\chi = 1.0$), is observed for all χ in (b) but for none in (c).

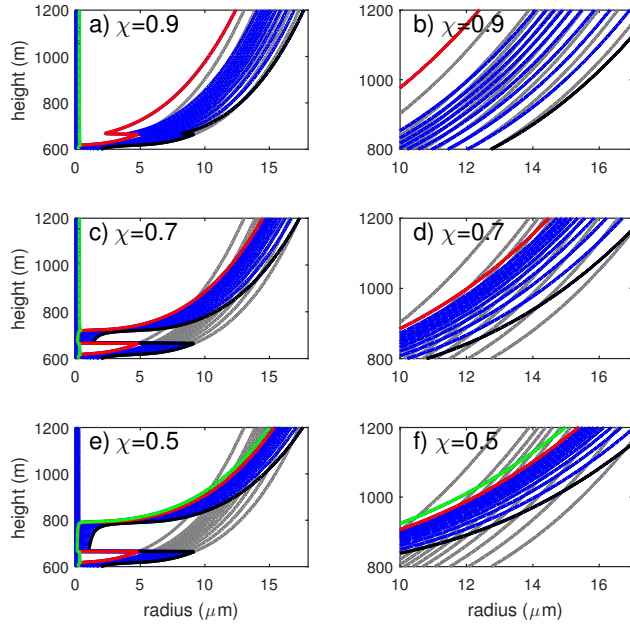


Figure 3. Radii of cloud droplets in a polydisperse population versus height for $\chi = 0.9, 0.7, 0.5$ in a clean environment at $w = 0.1 \text{ m s}^{-1}$. The background grey lines represent $\chi = 1.0$. The right column shows the region near the critical height where super-adiabatic growth can be expected. The black line is for the 1st bin (largest CCN), the red line for the 11th bin, and the green line for the 12th bin.

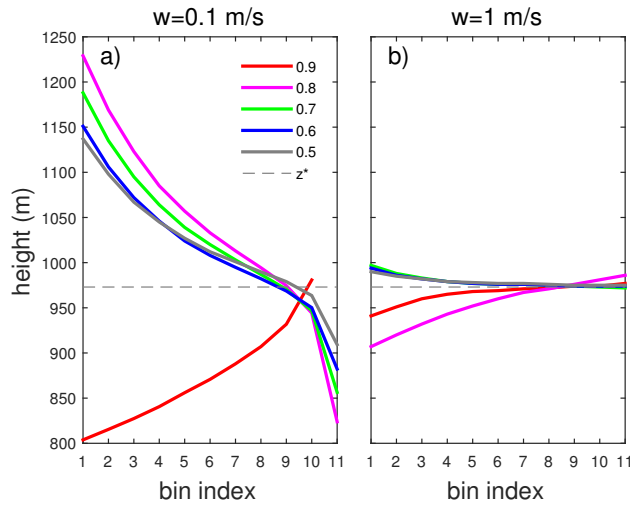


Figure 4. Critical height for individual droplet size bins for a polydisperse cloud droplet population calculated from cloud parcel model. Results are shown for two updraft velocities, (a) $w = 0.1 \text{ m s}^{-1}$ and (b) $w = 1.0 \text{ m s}^{-1}$. The line colors represent different mixing fractions χ as defined in the legend, and the dashed line is the analytical result for critical height z^* for a monodisperse cloud droplet population. Cloud droplet size decreases as the bin number increases.

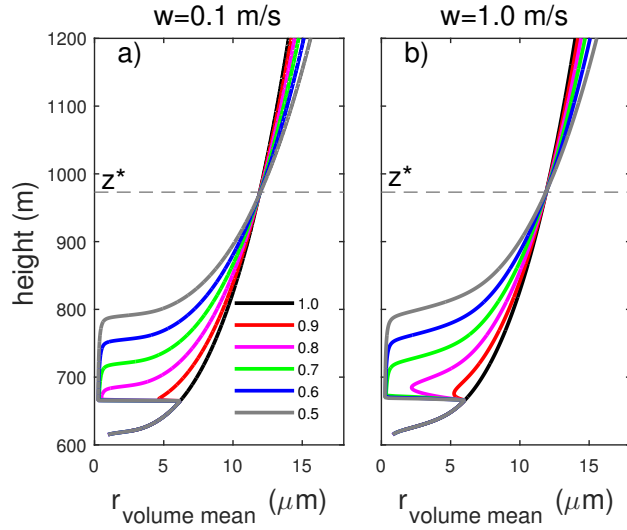


Figure 5. Volume-mean radius for a polydisperse cloud droplet population versus height at updraft speeds of a) $w = 0.1 \text{ m s}^{-1}$ and b) $w = 1.0 \text{ m s}^{-1}$ and for a clean environment. Line colors represent different mixing fractions χ , as in Figures 1 and 2. The horizontal dashed line is the critical height z^* predicted for a monodisperse cloud droplet population with equal volume-mean radius.

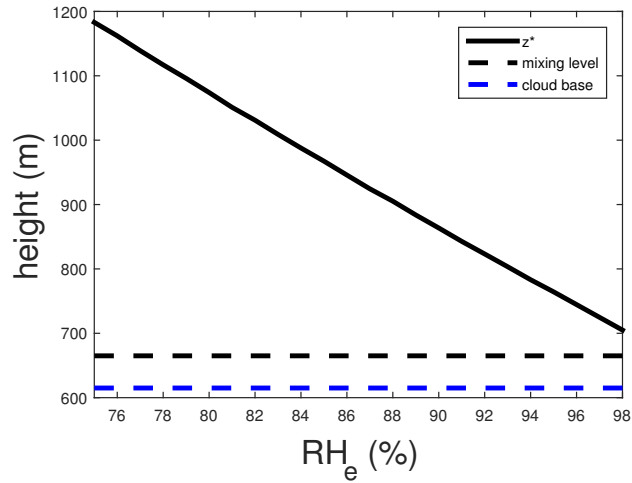


Figure 6. Critical height z^* versus environmental relative humidity RH_e at the mixing level. The height of cloud base (blue dashed line) and the mixing level (black dashed line) are shown for reference.